

PMMA/PPTA Microcomposites

M. Monleón Pradas,^{*,†} G. Schaber,^{†,‡} J. L. Gómez Ribelles,[†] and F. Romero Colomer[§]

Dept. de Termodinàmica Aplicada and Dept. de Física Aplicada, Universitat Politècnica de València, P.O. Box 22012, E-46071 Valencia, Spain

Received March 14, 1996; Revised Manuscript Received November 6, 1996[®]

ABSTRACT: Polymer composites of several concentrations of poly(methyl methacrylate) and poly(*p*-phenyleneterephthalamide) microfibrils have been prepared by blending a solution of the matrix polymer and a suspension of microfibrils obtained from a solution of commercial Kevlar fiber in H₂SO₄. Scanning electron microscopy shows that a continuous network of fibrils with dimensions in the range 30–70 nm builds up starting at very low PPTA concentrations and that these fibrils tend to form larger globular aggregates at higher PPTA concentrations. The high connectivity of the network is reflected in the good reinforcing effect as shown by the values of the dynamic-mechanical storage modulus. Increased interaction between the constituent phases as the fiber content grows is revealed by an increase of the calorimetric glass transition temperature and by thermogravimetric analysis, as well as by the growth of the slope of the Arrhenius plot of the main relaxation. The induced modifications of the matrix polymer's dynamic-mechanical spectrum are discussed with the help of predictions of a modified block model. A consistent interpretation of the temperature shifts of the glass transition and the main dynamic-mechanical dispersion can be gained on this basis. The numerical values of the model parameters that fit the experimental behavior correlate well with the buildup of structure revealed in the micrographs.

1. Introduction

The study here presented refers to what are sometimes called "molecular composites", but for reasons to become apparent, we prefer to call them "microcomposites". The concept of a molecular composite seems to have originated in the early 80s,^{1–3} and many attempts to approach the originally declared goals have been since then undertaken.^{4,5} The idea is to extend the principles of reinforcement employed in standard composite materials to a finer, "molecular" scale by means of a dispersion of rigid rod-like molecules in a ductile polymer matrix. An enhanced reinforcing efficiency should obtain both due to micromechanical reasons (the high aspect ratio due to the reduction to a molecular size of the fiber diameter) and as a consequence of the increased fraction of tie molecules,² which results in the case of having, instead of a macroscopic fiber, the same amount of reinforcing agent in the form of finely dispersed microfibrils. The dispersion of the rod-like molecules itself can be achieved either by blending solutions of both polymers,^{2,6–9} by graft copolymerization,^{2,10–12} or, more recently, by *in situ* rod formation techniques.⁵ Ideally, reinforcement should be at a maximum in the case of a homogeneous dispersion of the microfibrils in the matrix, but this situation is practically never achieved because of the high aggregation tendency¹² of the rod-like molecules: hydrogen bonding of the molecules themselves and a low entropy of mixing of the system rigid rod/flexible matrix coils cause the composite to phase separate. The resulting structures of the reinforcing phase then range in dimension from some tens of nanometers to micrometers. This is why "microcomposites" seems a preferable designation for this sort of materials.

Several ways to counterbalance the incompatibility of coils and rods have been attempted; one of them is

the enhancement of interactions (hydrogen bonding) between the rod-like molecules and the matrix molecules in order to favour the free energy of mixing.^{8,9} A case in which strong polar interactions between reinforcement and matrix has been reported is the (conventional) short-cut fiber composite system of poly(*p*-phenyleneterephthalamide)/poly(methyl methacrylate),^{13–15} PPTA/PMMA. The interaction between the amide groups of PPTA and the polar carboxyl groups of PMMA was advanced in refs 13–15 as the cause of a new α' relaxation process, which occurred after the main α relaxation of the matrix. This would be a genuine manifestation of a true interphase. Such an α' relaxation was also observed in the (conventional) composite system of PPTA continuous fiber and poly(ethyl methacrylate) matrix,¹⁶ but could not be obtained in the PPTA/PMMA continuous fiber composite.¹⁷ In these references we were led to an alternative explanation for the occurrence of such "new" peaks (see, below, the Discussion section). In any case, should new relaxation processes arise as a consequence of this specific polar interaction between the matrix polymer and the PPTA molecules, it is clear that they would be enhanced by an increase in the specific contact area of both constituents. Hence they should be clearly detectable in "molecular composites" of these materials. These reasons suggested the present investigation on PPTA/PMMA microcomposites, as well as a forthcoming one on the analogous PPTA/PEMA system.

2. Materials and Methods

a. Sample Preparation. Poly(methyl methacrylate) (PMMA) from Polysciences Ltd ($M_w = 350\,000$, density = 1.20), in the form of beads as received, was dried in vacuo for 24 h at 120 °C and then dissolved in tetrahydrofuran (THF) at ambient temperature to a 3% in weight concentration.

The source of poly(*p*-phenyleneterephthalamide) (PPTA) was commercial Kevlar 49 continuous fiber from Du Pont (density = 1.45). A suspension of PPTA fibrils in THF was prepared as follows.¹⁸ The fibers as received were dried in vacuo for 24 h at 120 °C, and then completely dissolved in H₂SO₄ for 48 h at 60 °C to a 0.5% in weight solution. Magnetic stirring and reflux condensation was employed in all the operations of solving and washing described in the present

* To whom correspondence should be addressed. Tel.: +(34 6)-3877324, e-mail: mmonleon@upvnet.upv.es.

[†] Dept. de Termodinàmica Aplicada.

[‡] Graduate student, FH Aalen, Aalen, Germany.

[§] Dept. de Física Aplicada.

[®] Abstract published in *Advance ACS Abstracts*, May 1, 1997.

section. Acetone was added to the PPTA/H₂SO₄ solution to precipitate PPTA in the form of a suspension which was subsequently filtered. The resulting "wet" PPTA powder was washed in acetone for 24 h at 60 °C and again filtered, and this operation was repeated three times. Then acetone was replaced by THF by the same method of repeated filtration and washing in THF. The final outcome had the appearance of a very fine white powder suspended in the liquid that did not precipitate.

Composite samples of PMMA/PPTA were prepared by casting mixtures of different proportions of the THF solutions of both species, after hours of homogenization by stirring, onto Petri dishes. In order to avoid the formation of bubbles, THF was evaporated slowly at ambient temperature until the sample seemed "dry". The samples were subsequently dried in vacuo over 4 days, increasing stepwise the temperature to 60, 95, and, finally, 125 °C, until the weight of the sample remained constant.

The films thus formed at the bottom of the Petri shells were then pressed between glass plates at 150 °C. Samples with thicknesses between 0.17 and 0.3 mm resulted, from which homogeneous pieces were cut for the measurements.

The procedure described ensured the absence of residuals of solvents in the composite samples. The presence of traces of H₂SO₄ was easy to detect, since it always resulted in the darkening of the samples when heated. Traces of THF could be detected in the thermogravimetry, as a small loss of weight at low temperatures. Only samples for which no residuals of either H₂SO₄ or THF could be detected were employed in the study.

The PPTA weight fraction in the composites was determined from the thermogravimetry of pieces cut from the samples. Since at 410 °C all pure PMMA was degraded (weight loss 100%) and no degradation of pure PPTA occurred below 480 °C, the remaining weight fraction of the composite samples at the temperature of 440 °C was accepted as the PPTA weight fraction. Results on samples of fiber weight fractions $\phi_w = 0$ (pure PMMA), 0.03, 0.10, 0.17, 0.33, 0.53, 0.69, and 1.00 (pure PPTA) are presented in this work.

b. Techniques. Scanning electron microscopy was performed in a Jeol JSM-6300 apparatus. The samples were frozen in liquid nitrogen and broken; the resulting surface was immersed in tetrahydrofuran for 5 min to remove the matrix polymer at the surface, and afterward it was gold metallized.

Thermal analysis was carried out in a Du Pont TGA 951 thermogravimetric apparatus. Weight loss against temperature was measured at a rate of 10 K/min in nitrogen flux, from 35 to 900 °C. The samples had sizes of about 5–10 mg, and all measurements were repeated twice. Of compositions $\phi_w = 0$ and 1.00 (both pure components) two samples were measured, one of the polymer as received (dried) and the other of the polymer films as they resulted from the preparation procedure described above.

A Perkin-Elmer DSC 4 differential scanning calorimeter was employed to measure the calorimetric glass transitions. The encapsulated samples were first heated in the apparatus up to 150 °C and kept at this temperature for 5 min in order to erase previous memory. Then they were cooled down to 60 °C at a rate of 40 K/min, and the measuring scan started at this temperature up to 150 °C, at a heating rate of 10 K/min.

Dynamic-mechanical spectroscopy was performed in a Polymer Laboratories DMTA-II apparatus, in the multifrequency heating scan mode, with a rate of 1 K/min. Frequencies measured were 0.3, 1, 3, 10, and 20 Hz, and the scan started at 25 and ended at 160 °C. The measurements were done in the single cantilever mode with a free length of 1 mm because of the small thicknesses of the samples. Since this small length is known to result in lower values of the storage modulus determined by the apparatus and no correcting formula was employed to account for this effect, an independent measurement of the storage moduli of all samples with a free length of 6 mm in the double cantilever mode was performed at room temperature in order to obtain a better estimate of the actual absolute value of E' .

3. Results

Figure 1 shows electron scanning micrographs for samples of $\phi_w = 0.03, 0.10, 0.17, 0.33, 0.53, 0.69$, and 1.00 (pure PPTA film obtained from the suspension of fibrils). A spatially connected network of fibril aggregates is already formed throughout the sample at the PPTA fraction of 0.10, with links having linear cross-sectional dimensions on the order of 30–70 nm. As the fiber fraction is increased, the network persists and becomes more dense, while its links grow tending to develop globular-shaped aggregates. For ϕ_w lower than 0.10, no macroscopically homogeneous samples could be obtained, and in these samples visible domains of pure PMMA coexisted with others in which the mixture PMMA/PPTA was more intimate and macroscopically homogeneous, as for $\phi_w \geq 0.10$. For this reason, no further measurements were performed on samples with $\phi_w < 0.10$. The micrograph shown in Figure 1a of the sample with $\phi_w = 0.03$ shows that the network, though already present, is less homogeneous than for the higher PPTA fractions and is even discontinuous throughout the sample.

Thermogravimetry of pure PMMA and PPTA samples is shown in Figure 2, parts a and b. Differences between degradation of commercial Kevlar 49 fiber and the film of PPTA fibrils prepared in this work are minimal, and both degradation curves show the pattern typical of PPTA.¹⁹ Degradation of pure PMMA seems to proceed in two stages, as suggested by the two peaks of the derivative curve, due probably to degradation of different molecular weight fractions of the polymer or to irregularities in the polymer (see, *e.g.*, ref 20 for the same situation in some methacrylate copolymers). The first of those peaks is depressed in the prepared polymer. The curve of thermal degradation shown in Figure 2(iii) for the $\phi_w = 0.33$ microcomposite is typical for all compositions. The two clearly separated loss processes correspond to the degradation of the two components. The temperatures of the peaks in the derivative curves (weight loss per temperature degree) corresponding to both components depend on sample composition as shown in Table 1, where an increase of the temperatures of both maxima as ϕ_w grows can be observed. The same tendency is also true for the onset of degradation, here arbitrarily represented by the temperature at which 0.01 of the weight is lost (Table 1).

PPTA shows no calorimetric transition in the temperature interval studied. Thus, the glass transition detected in DSC corresponds to the PMMA phase in the composite samples. The calorimetric glass transition temperatures of the samples, determined as the temperature corresponding to half the heat capacity increment in the transition, are shown in Table 1. As the PPTA content increases the glass transition temperature of the PMMA phase does also increase. The T_g increment between the $\phi_w = 0.69$ sample and the pure PMMA is something more than 10 °C.

Figure 3 shows the values of the dynamic-mechanical loss angle ($\tan \delta$) as a function of temperature at the fixed frequency of 1 Hz for all the samples measured. Values of $\tan \delta$ for pure PPTA microfibril film are almost constant and equal to 0.03 (the accepted value of PPTA fiber) in this temperature region, and no clear relaxation can be detected. Since a water-content dependent relaxation is known to occur¹⁹ around 60 °C, which disappears in dry PPTA, its absence in our measurements can be taken as a further indication of

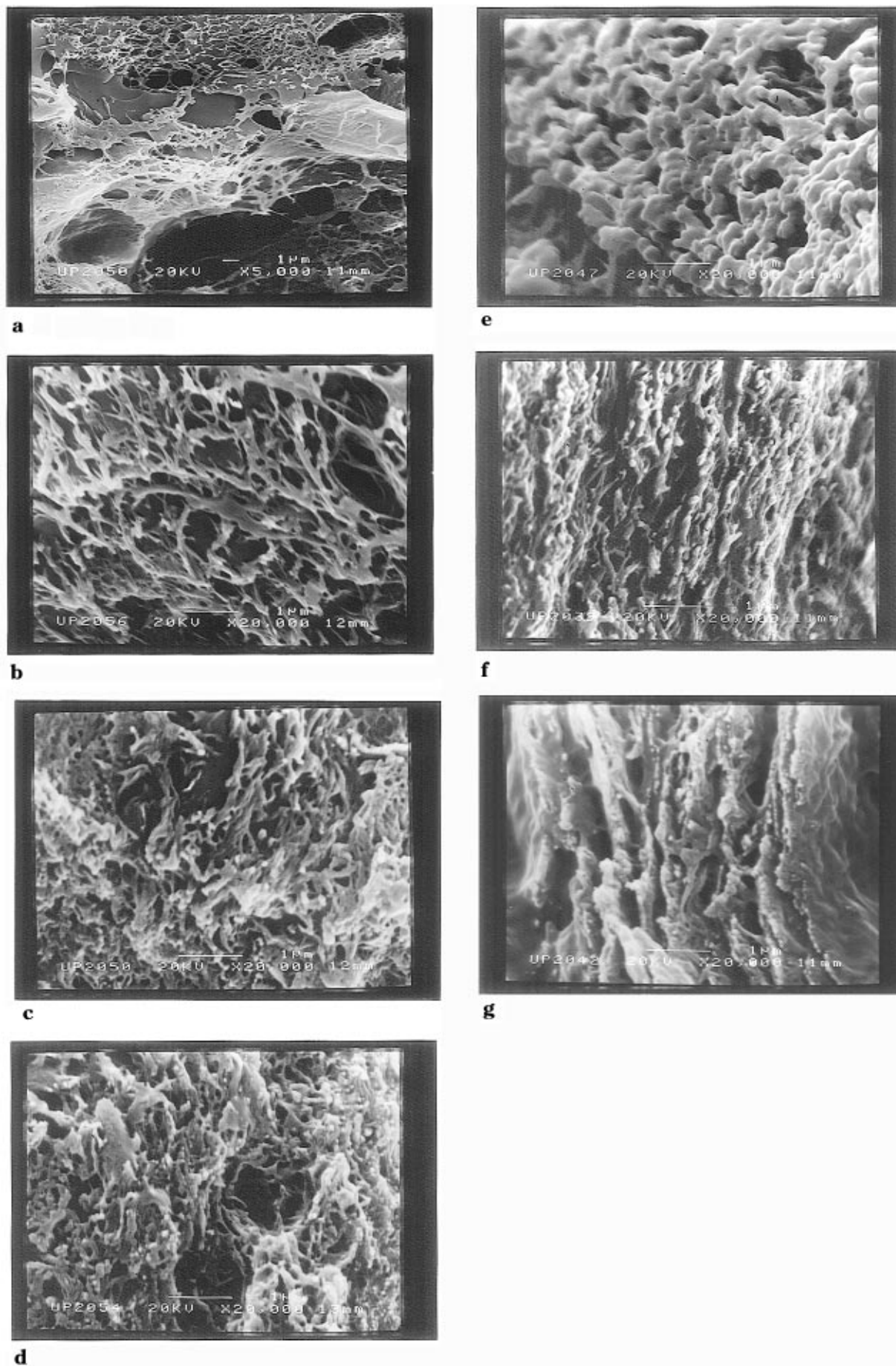


Figure 1. Scanning electron micrographs of PMMA/PPTA microcomposites of PPTA weight fractions ϕ_w equal to 0.03 (a), 0.10 (b), 0.17 (c), 0.33 (d), 0.53 (e), 0.69 (f), and 1.00 (g).

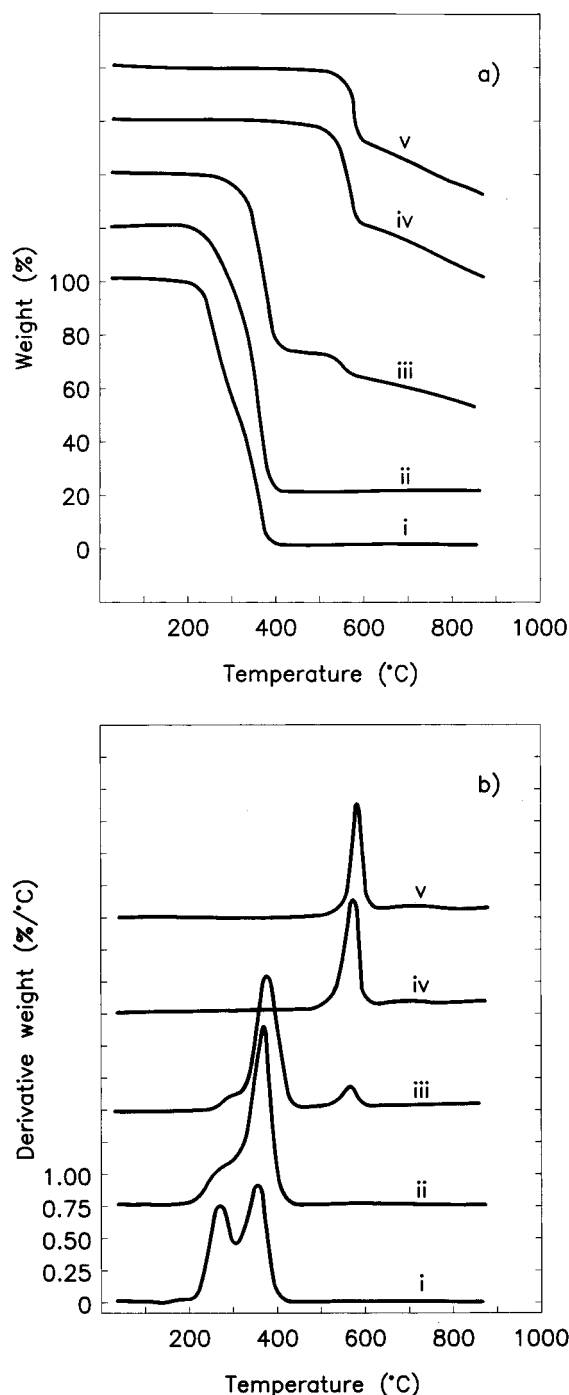


Figure 2. Thermogravimetric analysis of pure PMMA, pure PPTA, and $\phi_w = 0.33$ microcomposite showing (a) weight loss and (b) the temperature derivative of the weight loss: (i) PMMA as received; (ii) PMMA as prepared after dissolution; (iii) $\phi_w = 0.33$ microcomposite; (iv) pure PPTA microfibril mesh, as prepared; (v) pure PPTA as commercial Kevlar 49 fiber. Curves (ii–v) have been vertically displaced.

the absence of moisture. Pure PMMA exhibits its main relaxation process, the α relaxation, in the temperature interval studied. The peak showing up in the microcomposites corresponds to this main dispersion of the PMMA phase in the samples. As the PPTA content increases, the intensity of the α relaxation steadily decreases, whereas the temperature of the peak is shifted first to higher and then to lower temperatures. Figure 4 gives the storage moduli at 1 Hz and room temperature, showing the reinforcing effect of the PPTA fibril network. Figure 5 further shows the temperature course of the normalized storage modulus, $E'(T)/E'_{\max}$,

Table 1. Thermal Properties of the Microcomposites^a

ϕ_w	0	0.10	0.17	0.33	0.53	0.69	1.00
T_g	111.5	119.5	119	121	121.5	122	—
$\Delta C_p(T_g)$	0.247	0.251	0.251	0.270	0.244	0.225	—
T_{99}	228	279	270	276	254	276	453
T_{PMMA}^p	371	376	379	383	392	381	—
T_{PPTA}^p	—	558	558	566	576	580	575
E_a	430	370	420	480	480	510	—

^a Key: glass transition temperatures, T_g ; heat capacity jump at the glass transition, $\Delta C_p(T_g)$, referred to the PMMA weight in the sample, in J/g of PMMA; temperature at which 0.01 of the initial weight has been lost in TGA (T_{99}); peak temperatures for PMMA (T_{PMMA}^p) and for PPTA (T_{PPTA}^p) of the derivative of the thermal degradation curve. All temperatures are in °C, and the mean value of two measurements for each composition is given. Also, the apparent activation energy E_a (kJ/mol) of the main dynamic-mechanical relaxation is given.

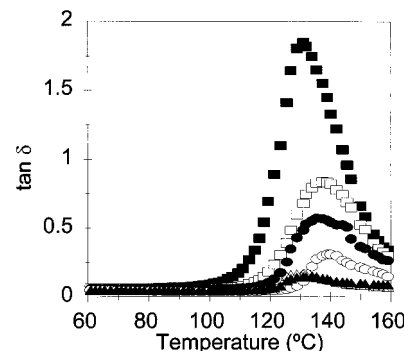


Figure 3. Values of $\tan \delta$ for the different microcomposites at 1 Hz as a function of temperature: (■) pure PMMA; (□) $\phi_w = 0.10$; (●) $\phi_w = 0.17$; (○) $\phi_w = 0.33$; (▲) $\phi_w = 0.53$; (△) $\phi_w = 0.69$.

at 1 Hz. With increasing ϕ_w the amplitude of the relaxation decreases, which is also shown in Figure 4. Normalization was chosen for this representation in order to minimize the effect of the scatter in the measurement of the samples' dimensions on the storage modulus values. This scatter is expected due to the small dimensions and to the inhomogeneities in thickness which may be unavoidable because of the preparation procedure. The geometrical dimensions of the sample enter the calculations of the apparatus' software through an additive constant for $\log E'$ which influences the absolute value of the modulus, but not that of $\tan \delta$, and cancels in the quotients $E'(T)/E'_{\max}$.

4. Discussion

The above experimental results suggest that the PMMA/PPTA microcomposites prepared in this way can be considered "mesoscopically homogeneous" materials for PPTA contents higher than $\phi_w = 0.10$. It is meant by this that pieces in the typical size range of, e.g., those employed for conventional DSC or TGA measurements can be picked at random from the prepared sample, and they appear macroscopically homogeneous (while this would be untrue for $\phi_w = 0.03$, for example). Microscopically, nevertheless, these composites consist of two separate phases, which evidence suggests a co-continuous nature, with one of them in the form of a spatially connected network, as found also in PPTA/nylon microcomposites.⁷ In contrast with that system, nevertheless, in our case even the 0.03 sample is phase-separated (whereas ref 7 reports a single homogeneous phase for PPTA weight contents up to 0.10). This contrast can be due to the different modes of preparation. Early work on rigid-rod-based molecular composites already

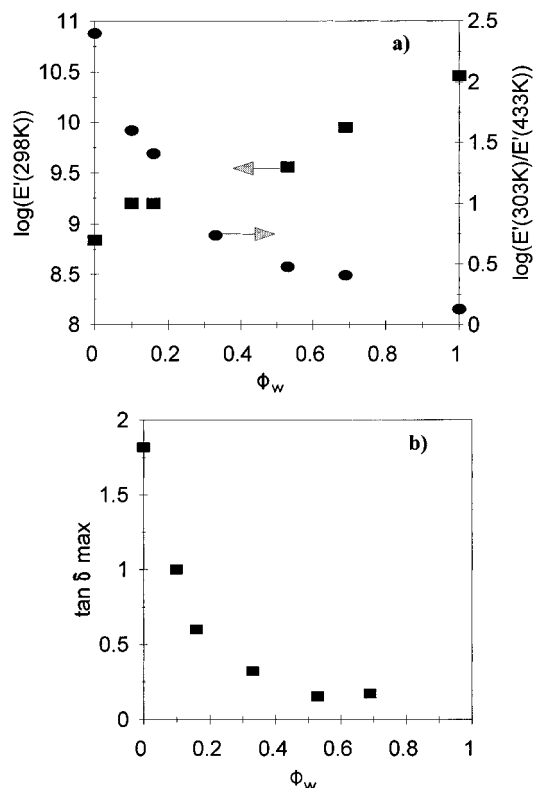


Figure 4. (a) Absolute value of the storage modulus E' at room temperature (■) and of the relative modulus fall, $E'(303\text{ K})/E'(433\text{ K})$ (●). (b) Value of the maximum of $\tan \delta$. All results are at 1 Hz, as functions of the PPTA weight content in the microcomposites.

showed that a microfibril network is formed once the fibrils are formed and redissolved.^{1,3} Scanning electron micrographs show the progressive build-up of the network as the PPTA content grows, from a still not fully developed and discontinuous stage ($\phi_w = 0.03$) to a fully continuous structure ($\phi_w \geq 0.10$) throughout the sample. The linking elements of this structure become appreciably larger from a certain PPTA content upward ($\phi_w = 0.33$), with a globulelike appearance. These larger aggregates become more densely packed as ϕ_w increases further. That the network formed has a high connectivity is reflected in the high values of the dynamic-mechanical storage modulus, Figure 4. A comparison between the decrease of the normalized storage modulus and of $\tan \delta$ of the present microcomposites (Figures 4 and 5), on one hand, and the same quantities of PMMA/Kevlar 49 continuous fiber composites (Figures 1a, 6, and 7 of our earlier ref 17), on the other hand, shows that the same decreases are obtained in both cases for PPTA contents greater than 0.17, *i.e.*, when the network structure can be considered fully developed. In this respect, the reinforcement by the PPTA microfibril network seems to be as efficient as that of *continuous* parallel fibers.

The fact that the PPTA phase has this three-dimensional extended networklike structure even at very low contents (and does not, for example, result in finely dispersed unconnected inclusions) must be attributed to the rigid rod-like nature of the PPTA molecular aggregates when in the solvated state and their large linear dimension.²¹ Comparing our SEM findings with the known hierarchical supramolecular structure of the Kevlar 49 fiber,^{22,21} the elementary units originating in the $\text{H}_2\text{SO}_4/\text{PPTA}$ solution which constitute the basic building blocks of the links in the

network appear to be microfibrils of diameter in the range between 10 nm (as reported in ref 18; in ref 2, figures of 15–30 nm are given) and 70 nm. Bundles of 60 nm diameter cylindrical crystallites have been proposed as the structure of the elementary Kevlar fiber;²³ these bundles phase separate when the fiber is hydrolytically degraded.^{21,24} Strong hydrogen bonding between the $-\text{NH}$ and $-\text{CO}$ groups of molecules in adjacent microfibrils would account for the prominent aggregation tendency of these into larger formations. The strength of these bondings between microfibrils and their aggregates, as well as the connectivity of the resulting network, is evidenced in the high storage modulus of the pure PPTA film prepared, $\log E' (\text{Pa}) = 10.4$ (Figure 4), that of Kevlar 49 continuous fiber being 11.2. Dramatic improvements of strength with the increase of microfibril content have been reported in acrylate-based latexes/cellulose nanocomposites and have been also attributed to the hydrogen bonding of the microfibrils and their connection through percolation.²⁵

The experimental results show features which can be interpreted as indications of a strong interaction between the PPTA phase and the PMMA phase. The TGA data (Figure 2 and Table 1) tell about an increase in the thermal stability of the microcomposites, reflected²⁰ in the shift towards higher values of the significant degradation temperatures. The displacement towards higher temperatures of the glass transition temperature of the PMMA phase of the microcomposites (Table 1) is also indicative of enhanced interaction between the component species and has also been found in ref 6. The same is suggested by the Arrhenius plots (logarithm of the frequency *versus*/ reciprocal of the peak temperature at each frequency) of the main dynamic-mechanical dispersion process for each composite. The slopes of these plots, interpreted as an apparent activation energy of the process, are given in Table 1. The clearly defined increasing trend with ϕ_w of the apparent activation energy must be related to increased hindering of the microbrownian motion of the PMMA chain segments originating the α relaxation. This hindrance may arise as a consequence of adsorption²⁶ of the PMMA molecules onto the microfibril mesh or as consequence of electrostatic interaction between the polar groups of the PMMA and PPTA molecules.^{13,14} This kind of interfacial interaction has been observed also between the Kevlar filament and Nylon 6 in ref 27. Besides these local restrictions due to specific molecular interactions, the increased motional difficulties for the PMMA main chain segments could also have a nonlocal nature, due to steric confinement of some portions of the PMMA phase in the cavities of the PPTA network. In this respect, the confined relaxation of the PMMA matrix in the network spaces left by the PPTA phase is similar to the confined relaxation of other systems in micropores,²⁸ which also gives rise to the phenomenology here encountered (shifts in T_g 's, increased activation energies). This is usually discussed in terms of the notion of "cooperativity length", the characteristic length of the cooperative processes of the main relaxation, and its relative size with respect to the confining length. The interaction of the matrix polymer chains with the reinforcing phase may thus lead to the formation of a boundary layer,²⁶ or mesophase,^{29,30} of PMMA molecules with restricted mobility; the regions of "tightly bound" and "loosely bound" polymer³¹ can thus have different thermomechanical behaviors. Lipatov's theory employs

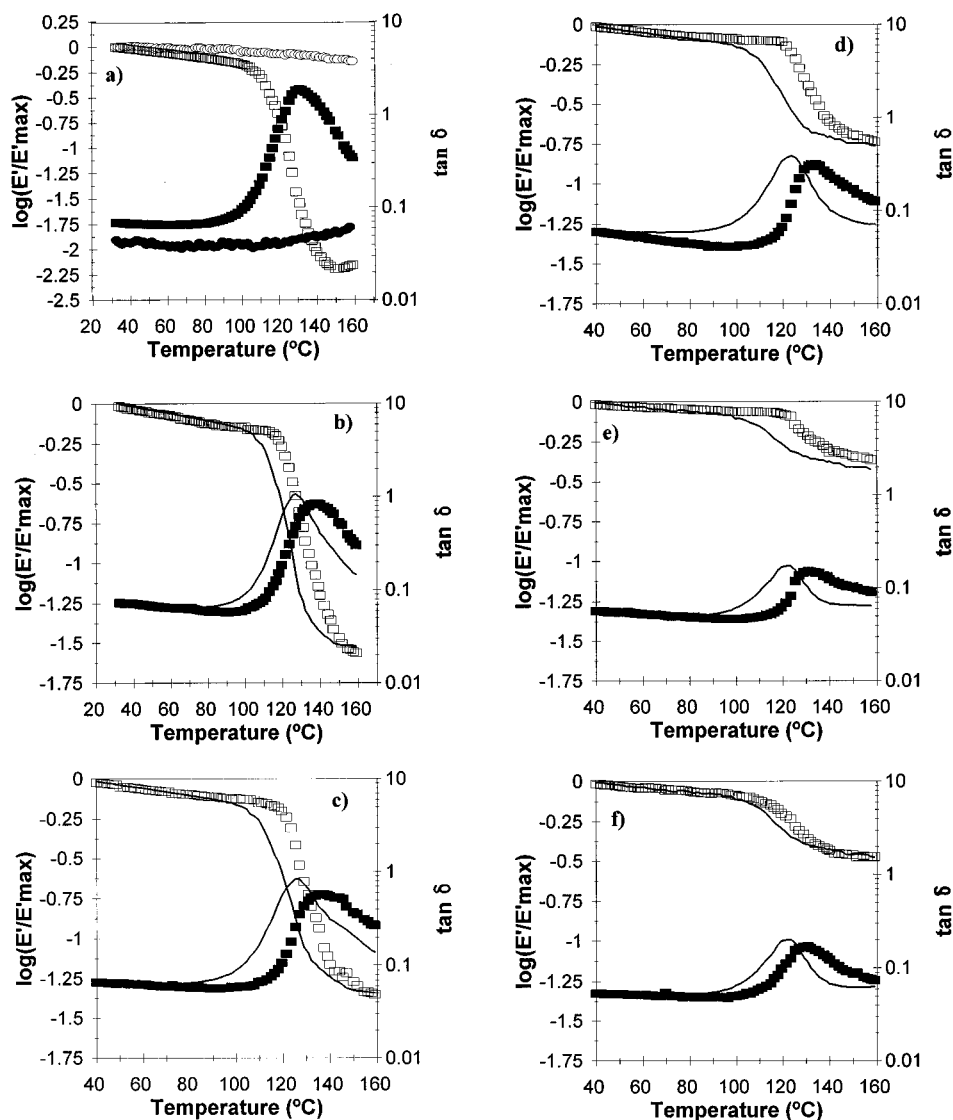


Figure 5. Logarithm of the normalized storage modulus $\log(E(T)/E_{\max})$ and $\tan \delta(T)$ at 1 Hz versus temperature T for the different compositions. Symbols are the experimental results; the solid lines are the model equations' predictions. Key: (a) pure components (PMMA boxes, PPTA circles); (b) $\phi_w = 0.10$; (c) $\phi_w = 0.17$; (d) $\phi_w = 0.33$; (e) $\phi_w = 0.53$; (f) $\phi_w = 0.69$.

as a measure f of the fraction of matrix polymer chains whose mobility is restricted at the boundary interphase in a composite of ϕ_w the quotient of specific heat capacity jumps at the glass transition, $f = 1 - \Delta c_p(\phi_w)/\Delta c_p(0)$; for spherical inclusions the thickness of the boundary layer can then be deduced.²⁶ In Table 1 we give the $\Delta c_p(\phi_w)$ data for our samples, referred to the PMMA weight in each sample. Constancy of these values should be expected if the thermal behavior of PMMA remained unaffected by the presence of the PPTA phase. On the contrary, the increase in configurational degrees of freedom translated by $\Delta c_p(T_g)$ should be less in samples with restricted mobility of the polymer chains than in pure PMMA. This last effect is observed clearly only in the samples of greater PPTA content but is less evident in the rest of the samples.

Although modifications of the PMMA behavior caused by interactions with the PPTA phase are thus clearly evidenced by the measurements undertaken in the present study, they nevertheless did not lead to the occurrence of a new α' relaxation, attributable to an interphase,^{26,31} as happened in refs 13 and 14.

The only experimental data that seem at variance with the tendency commented on in the last paragraph are the temperature shifts of the $\tan \delta$ peaks in the

dynamic-mechanical measurements, Figure 3. In fact, they first increase but then, for $\phi_w \geq 0.17$, start decreasing, in contrast with the dependence of T_g on ϕ_w (Table 1). However, a closer analysis shows why indeed this should be so.

In earlier papers^{16,17,32} we have cautioned against an immediate interpretation of the shifts of the peaks of the dynamic-mechanical spectra, or even of the occurrence of new peaks in such spectra of heterogeneous materials, as by themselves implying modifications in the component materials relaxational behavior. There we pointed out that, in some cases, these changes in the measured spectra do not correspond to genuine changes in the properties of the phases but are simply the overall thermomechanical response of a two-phase material when one of the phases does not relax. Temperature shifts in the other phase's relaxation and even new peaks, absent from the spectra of both pure phases, can be generated in this way, not corresponding to any true change in the behaviour of the component polymer. These effects are best sorted out by looking at the overall behaviour predicted by a model which determines the dynamic-mechanical properties of the composite in terms of the properties of the *pure*, unmodified components.

Table 2. Temperature Shifts $\Delta T_{\alpha} = T_{\alpha}(\phi_w) - T_{\alpha}(\phi_w = 0)$ of the Maximum at 1 Hz of $\tan \delta$ as a Function of PPTA Weight Fraction ϕ_w^a

	ϕ_w 0.10	ϕ_w 0.17	ϕ_w 0.33	ϕ_w 0.53	ϕ_w 0.69
$\Delta T_{\alpha}^{\text{exp}}$	7	4	0.5	-1	-1
$\Delta T_{\alpha}^{\text{mod}}$	-6	-7	-8.5	-10	-10
$\Delta T_{\alpha}^{\text{corr}}$	2	0.5	1	0	0.5

^a Key: first row, experimental values; second row, values predicted by the model; third row, model prediction corrected by adding to the values of the second row the calorimetrically determined shift in T_g , $\Delta T_g(\phi_w) = T_g(\phi_w) - T_g(\phi_w = 0)$, from Table 1.

In the present work, as in our earlier refs 16, 17, and 32, we have employed a modification of Takayanagi's parallel-series three-block model,^{26,33} consisting of two blocks in parallel, one for PMMA and one for PPTA, working in series with a third block, again of PMMA. The experimentally measured behaviour of each *pure* component is assigned to the respective blocks. The volume fraction of PPTA (*i.e.*, volume fraction of the second block), ϕ , is determined from the corresponding ϕ_w values and the polymers' densities, while the volume fraction of the PMMA block in series λ and a coefficient of effectiveness K affecting multiplicatively the complex modulus of the reinforcement are regarded as the adjustable parameters of the model (the model equations and a discussion of the physical meaning attributed to λ and K can be found in any of the just mentioned references and are not repeated here). The model is then fitted to the experimental behavior, and the values of these parameters are determined. Figure 5b-f shows this fit for each composition, while Figure 5a gives the behaviour of pure PMMA and PPTA (as prepared) fed as data into the model. It can be appreciated that the shape of the curves and both the height of $\tan \delta$ and the fall of the normalized storage modulus can be well reproduced, but the temperatures of the dispersion region are systematically displaced towards *lower* values and are impossible to adjust. Thus, on the basis of the properties of the pure polymers, a shift towards lower temperatures of the main relaxation is predicted as ϕ increases, due to the overall behavior and not to changes in the phases' properties. These shifts are larger than those experimentally measured. If now we recall that changes in the PMMA phase have indeed taken place in the microcomposites, changes not accounted for in the model calculations, we may correct the latter's predictions as shown in Table 2: if the experimental shift in the glass transition temperature ΔT_g is added to the shift in the temperature of the α peak predicted by the model, $\Delta T_{\alpha}^{\text{mod}}$, then the dependence on composition of $\Delta T_g + \Delta T_{\alpha}^{\text{mod}}$ has the same pattern as that of the experimental shift of T_{α} , $\Delta T_{\alpha}^{\text{exp}}$: it first increases and then, for $\phi_w > 0.1$, it starts decreasing. This means that also the dynamic-mechanical loss angle data are consistent with the discussion held in this section and that the pattern of the dependence on ϕ_w of the peak temperatures was the superposition of two effects, one of them being a genuine modification of the matrix properties and the other being simply caused by the heterogeneity of the relaxing system. This same situation has been found also in other polymer composites.³⁴

The build-up of the network is also reflected by the values of the model parameter λ (volume of PMMA in the series block divided by the total volume of PMMA in the composite sample) obtained for each composition. λ decreases with increasing ϕ_w with a pronounced step

at the fibril concentration at which the larger globular aggregates are completely developed: its value of 0.04 for $\phi_w = 0.1$ and $\phi_w = 0.17$ is more than 10-fold reduced to a value of 0.001 for $\phi_w = 0.33$ and stabilizes at 0.0005 for $\phi_w = 0.53$ and 0.69.

5. Conclusions

PMMA/PPTA molecular composites have been prepared by blending solutions of the matrix polymer and the finely dispersed microfibrils. The composites have a two-phase, cocontinuous morphology, the microfibril phase forming a highly connected three-dimensional network with transverse dimensions of its structural elements in the range of tens to hundreds of nanometers. An enhancement of interaction between the matrix and the fibril molecules is suggested by the increase with fibril concentration of such magnitudes as the calorimetric T_g , the activation energy of the main dynamic-mechanical relaxation, and the degradation temperature. Even if the formation of a matrix boundary interphase responsible for such observed changes can be hypothesized, no specific distinct relaxation of that interphase was detected, either by calorimetric or by dynamic-mechanical methods. The dynamic-mechanical spectra of the microcomposites could be consistently interpreted only after sorting out purely overall effects from genuine modification of the relaxation behavior through a comparison with the prediction of a simple modified block model. This analysis demonstrates that factors of a very diverse nature may merge in the experimentally measured dynamic-mechanical spectra of heterogeneous materials and that the use of models based on the properties of the pure homopolymers is *necessary* to discern which features originate in true interactions and which are simply due to overall effects. In thermodynamical terms, only the "excess" spectrum, determined as the difference between the experimental spectrum and that predicted by an ideal model, can be interpreted in terms of property changes of the component phases of the system caused by their interaction.

Acknowledgment. G.S. held an Erasmus grant while this work was performed. The work was supported by the Spanish CICYT through Project MAT 91-0578.

References and Notes

- (1) Helminiak, T. E.; Benner, C. L.; Arnold, F. E.; Husman, G. E. U.S. Patent 4207407, 1980.
- (2) Takayanagi, M.; Ogata, T. *J. Macromol. Sci.-Phys.* **1980**, B17, 591.
- (3) Hwang, W.-F.; Wiff, D. R.; Benner, C. L.; Helminiak, T. E. *J. Macromol. Sci.-Phys.* **1983**, B22, 231.
- (4) Schaefer, D. W.; Mark, J. E., Eds. *Polymer Based Molecular Composites*; Materials Research Society: Pittsburgh, PA, 1990.
- (5) Wiff, D. R.; Lenke, G. M.; Fleming, P. D., III. *J. Polym. Sci. B: Polym. Phys.* **1994**, 32, 2555.
- (6) Yamada, K.; Mitsutake, T.; Takayanagi, M.; Kajiyama, T. *J. Macromol. Sci.-Phys.* **1989**, A26, 891.
- (7) Park, H.-S.; Kyu, T. *Polym. Compos.* **1989**, 10, 429.
- (8) Painter, P. C.; Tang, W.-L.; Graf, J. F.; Thomson, B.; Coleman, M. M. *Macromolecules* **1991**, 24, 3929.
- (9) Dai, Y. K.; Chu, E. Y.; Xu, Z. S.; Pearce, E. M.; Okamoto, Y.; Kwei, T. K. *J. Polym. Sci. A: Polym. Chem.* **1994**, 32, 397.
- (10) Song, H. H.; Price, G. E.; Vakil, U. M.; Dotrong, M. H. *Polym. Prepr.* **1992**, 33 (1), 319.
- (11) Dotrong, M.; Dotrong, M. H.; Evers, R. C. *Polym. Prepr.* **1992**, 33 (1), 477.
- (12) Song, H. H.; Dotrong, M.; Price, G. E.; Dotrong, M. H.; Valkil, U. M.; Santosh, U.; Rivers, R. C. *Polymer* **1994**, 35, 675.

- (13) Kodama, M.; Karino, I. *J. Appl. Polym. Sci.* **1986**, *32*, 5057.
- (14) Kodama, M.; Karino, I. *J. Appl. Polym. Sci.* **1986**, *32*, 5345.
- (15) Kodama, M.; Karino, I.; Kuramoto, K. *Polym.-Plast. Technol. Eng.* **1988**, *27*, 127.
- (16) Gómez Ribelles, J. L.; Mañó Sebastià, J.; Martí Soler, R.; Monleón Pradas, M.; Ribes Greus, A.; Suay Antón, J. J. *J. Appl. Polym. Sci.* **1991**, *42*, 1647.
- (17) Díaz Calleja, R.; Gómez Ribelles, J. L.; Monleón Pradas, M.; Ribes Greus, A.; Romero Colomer, F. *Polym. Compos.* **1991**, *12*, 428.
- (18) Takayanagi, M.; Goto, K.; Yamada, K. *Rep. Prog. Polym. Phys. Jpn.* **1981**, *24*, 311.
- (19) Kunugi, T.; Watanabe, H.; Hashimoto, M. *J. Appl. Polym. Sci.* **1979**, *24*, 1039.
- (20) Choudhary, M. S.; Varma, I. K. *J. Macromol. Sci.-Chem.* **1983**, *A20*, 941.
- (21) Morgan, R. J.; Allred, R. E. In *International Encyclopedia for Composites*; Lee, S. M., Ed.; VCH Publishers: New York, 1990; Vol. 1, pp 37–56.
- (22) *Concise Encyclopedia of Composite Materials*; Kelly, A., Ed.; Pergamon Press: London, 1994; p 133.
- (23) Brown, I. M.; Sandreczki, T. C.; Morgan, R. J. *Polymer* **1984**, *25*, 759.
- (24) Morgan, R. J.; Pruneda, C. O. *Polymer* **1987**, *28*, 340.
- (25) Favier, V.; Cahnzy, H.; Cavaille, J. Y. *Macromolecules* **1995**, *28*, 6365.
- (26) Lipatov, Yu. S. *Adv. Polym. Sci.* **1977**, *22*, 1.
- (27) Kumamaru, F.; Oono, T.; Kajiyama, T.; Takayanagi, M. *Polym. Compos.* **1983**, *4*, 141.
- (28) Pissis, P.; Daoukaki-Diamanti, D.; Apekis, L.; Christodoulides, C. *J. Phys.: Condens. Matter* **1994**, *6*, L325.
- (29) Theocaris, P. S.; Spathis, G. D. *J. Appl. Polym. Sci.* **1982**, *27*, 3019.
- (30) Theocaris, P. S.; Ponirides, P. H. *J. Appl. Polym. Sci.* **1986**, *32*, 6267.
- (31) Tsagaropoulos, G.; Eisenberg, A. *Macromolecules* **1995**, *28*, 6067.
- (32) Gómez Ribelles, J. L.; Monleón Pradas, M.; Más Estellés, J.; Meseguer Dueñas, J. M.; Romero Colomer, F. *Plast., Rubber Compos. Proc. Appl.* **1992**, *18*, 169.
- (33) Takayanagi, M. *Mem. Fac. Eng. Kyushu Univ.* **1963**, *23*, 41.
- (34) Monleón Pradas, M.; Gómez Ribelles, J. L.; Vidaurre Garayo, A.; Más Estellés, J.; Romero Colomer, F.; Meseguer Dueñas, J. In *Progress and Trends in Rheology VI, Proceedings of the 4th European Rheology Conference*; Gallegos, C., Ed.; Steinkopff Verlag: Darmstadt, Germany, 1994; p 63.

MA9603847